PHYSICAL REVIEW D **79,** 064011 (2009)

Spherical scalar-tensor galaxy model

Jorge L. Cervantes-Cota,[1] Mario A. Rodríguez-Meza,[1] and Darío Núñez[2]

(Instituto Avanzado de Cosmología, IAC)

[1]*Depto. de Física, Instituto Nacional de Investigaciones Nucleares, Apdo. Postal 18-1027, México D.F. 11801, México*
[2]*Instituto de Ciencias Nucleares, Universidad Nacional Autónoma de México, A.P. 70-543, 04510 México D.F., México*
(Received 8 December 2008; published 16 March 2009)

We build a spherical halo model for galaxies using a general scalar-tensor theory of gravity in its Newtonian limit. The scalar field is described by a time-independent Klein-Gordon equation with a source that is coupled to the standard Poisson equation of Newtonian gravity. Our model, by construction, fits both the observed rotation velocities of stars in spirals and a typical luminosity profile. As a result, the form of the new Newtonian potential, the scalar field, and dark matter distribution in a galaxy are determined. Taking into account the constraints for the fundamental parameters of the theory (λ, α), we analyze the influence of the scalar field in the dark matter distribution, resulting in shallow density profiles in galactic centers.

DOI: 10.1103/PhysRevD.79.064011 PACS numbers: 04.50.−h, 04.25.Nx, 98.62.Gq, 98.62.Js

I. INTRODUCTION

The recent indirect observational evidence of dark matter (DM) and dark energy in the Universe [1–9] has motivated the study of new cosmological and astrophysical scenarios that can encompass these observations. At a cosmological level, the quintessence scenario [10–12] provides fittings to the present accelerated expansion rate of the Universe and should be consistent with the other abovementioned observations. Typically, quintessence introduces new fields that have their origin in theories that attempt to unify all forces of nature (strings, braneworlds). These unification schemes result in extensions to general relativity, which determine a new dynamics. Scalar-tensor theories (STT) of gravity are examples of effective theories that stem from such unifying schemes [13,14]. As one may suspect, in addition to cosmological consequences, such theoretical extensions also predict local, astrophysical effects. Traditionally, to understand the dynamics of a galaxy, a DM profile has been introduced[15] or, alternatively, a modification to the Newtonian gravitational law, e.g. via Yukawa couplings [16], or even modifications to the Newtonian motion law, such as MOdified Newtonian Dynamics [17,18]. Within the first approach, several DM candidates have been proposed, including a scalar field (SF) as DM itself [19,20]. The second approach has been used to obtain flat rotation curves in spirals via STT, without using DM halos. Adjusting rotation curve profiles using STT implies that the strength of the Yukawa coupling, α, has to be negative, leading to a phantomlike nonminimally coupled field. Moreover, the adjustment of different rotation curves of specific galaxies, points to different values for the range parameter of the theory, λ [21], implying a mass spectrum for the fundamental theory at hand. The third approach solves flat rotation curves dynamics in spirals, but fails to fully understand cluster dynamics. This latter approach will not be considered here. Our model is a combination of the first two approaches mentioned above: we use both a DM halo and a SF nonminimally coupled to general relativity, as long as these two elements could simultaneously play a role in the galactic dynamics, and mitigate the constraints imposed on STT parameters, when using that theory alone.

Following this line of thought, we have recently studied [22,23] the influence that STT have at galactic scales, see also [24]. We considered the Newtonian limit of STT and computed potential-density pairs of a spherical galaxy in which Navarro, Frenk, and White's (NFW) [25] and Dehnen's [26] density profiles were used. We also computed some other relevant observational quantities (rotation curves, dispersions), by which we accounted for the influence of the STT scalar fields in the Galaxy. Such influence is characterized by the two parameters (λ, α) of STT, see below. In this work we use this formalism to build a galactic model that is, by construction, consistent with the measured rotation curves of stars and with some luminosity profile. As a result, the form of the Newtonian potential is exactly solved, and the SF and DM distribution in a galaxy are numerically computed, and their specific features depend on the fundamental parameters (λ, α) of the STT. For the values of the parameter space analyzed, the resulting DM has shallow profiles near the center.

Some other models such as the gravitational suppression hypothesis [27] have been put forward, in which a Yukawa term is added in the Newtonian potential. Recently, [28] analyzed the rotation curves best fit in this model, in which a NFW profile is used. They concluded that this hypothesis does not fit several rotational curves of spirals and, hence, does not solve the core/cuspy problem of DM in the center of galaxies. Arguments in favor of a cusplike center can be

found in Refs. [29–33]; however, recently more evidence has emerged favoring a corelike galactic center [34–45]. In [46] a way can be found to reconcile both approaches.

The present work is organized as follows: in the next section we give a brief description of the STT Newtonian approximation, where the SF background value is set to have the usual gravitational constant value at small distances, $r \ll \lambda$. In Sec. III, we build a galactic model by giving the rotation curves and baryon density profile, and in Sec. IV we analyze the influence of the pair of parameters (λ, α) on the SF and DM density distributions. Finally, in the last section we discuss the results and present our conclusions.

II. THE NEWTONIAN APPROXIMATION OF STT

A typical STT is given by the following Lagrangian [47,48]:

$$\mathcal{L} = \frac{\sqrt{-g}}{16\pi}\left[-\phi R + \frac{\omega(\phi)}{\phi}(\partial\phi)^2 - V(\phi)\right] + \mathcal{L}_M(g_{\mu\nu}), \tag{1}$$

where $g_{\mu\nu}$ is the metric, ϕ is a SF, and $\omega(\phi)$ and $V(\phi)$ are arbitrary functions of it. $\mathcal{L}_M(g_{\mu\nu})$ is the matter Lagrangian. From Eq. (1) one obtains the gravity and SF equations. Thus, the gravitational equation is

$$R_{\mu\nu} - \frac{1}{2}g_{\mu\nu}R = \frac{1}{\phi}\left[8\pi T_{\mu\nu} + \frac{1}{2}V(\phi)g_{\mu\nu} + \frac{\omega(\phi)}{\phi}\partial_\mu\phi\partial_\nu\phi - \frac{1}{2}\frac{\omega(\phi)}{\phi}(\partial_\mu\phi)^2 g_{\mu\nu} + \phi_{;\mu\nu} - g_{\mu\nu}\Box\phi\right]. \tag{2}$$

The SF Klein-Gordon equation is

$$\Box\phi + \frac{\phi V' - 2V}{3+2\omega} = \frac{1}{3+2\omega}[8\pi T - \omega'(\partial\phi)^2], \tag{3}$$

where a prime (') denotes the derivative with respect to SF.

In accordance with the Newtonian approximation, gravity and SF are weak. Then, we expect to have small deviations of the SF around the background field. Assuming also that the velocities of stars and DM particles are nonrelativistic, we perform the expansion of the field equations around the background quantities $\langle\phi\rangle$ and $\eta_{\mu\nu}$, i.e., $g_{\mu\nu} = \eta_{\mu\nu} + h_{\mu\nu}$ and $\phi = \langle\phi\rangle + \delta\phi$.

The equations governing the weak energy (Newtonian) limit of STT are well known [22,49–52] and written here in physical units ($h \neq 1, c \neq 1$)

$$\frac{1}{2}\nabla^2 h_{00} = \frac{G_N}{(1+\alpha)c^2}\left[4\pi\rho - \frac{1}{2}\nabla^2\delta\phi\right], \tag{4}$$

$$\nabla^2\delta\phi - \left(\frac{mc}{h}\right)^2\delta\phi = -8\pi\alpha\rho, \tag{5}$$

where the background value is chosen such as $\langle\phi\rangle = (1+\alpha)c^2/G_N$, a choice that sets the effective Newtonian constant to the one locally observed, see [49,53] for a detailed discussion. Equations (4) and (5) represent the Newtonian limit of a set of STT that are distinguished by the effective square mass $m^2 \equiv \alpha(\langle\phi\rangle V''_{\phi=\langle\phi\rangle} - V'_{\phi=\langle\phi\rangle}) - 2\alpha^2\omega'_{\phi=\langle\phi\rangle}(\langle\phi\rangle V'_{\phi=\langle\phi\rangle} - 2V_{\phi=\langle\phi\rangle})$ and $\alpha \equiv 1/(3+2\omega(\phi))\,|_{\phi=\langle\phi\rangle}$; $\omega(\phi)$ is a generalization of the Brans-Dicke parameter [47].

In the above expansion we have set the cosmological constant equal to zero since within galactic scales its influence is negligible. This is because the average density in a galaxy is much larger than a cosmological constant that is compatible with observations. Thus, we only consider the influence of luminous and dark matter. These matter components gravitate in accordance with the modified-Newtonian theory determined by Eqs. (4) and (5). The latter is a Klein-Gordon equation, which contains the boson field of mass m, whose Compton wavelength ($\lambda = h/mc$) implies a length scale for the new dynamics. We shall assume this scale to be of the order of kiloparsecs.

Note that Eq. (4) can be cast as a Poisson equation for $\psi \equiv \frac{c^2}{2}(h_{00} + \frac{\delta\phi}{\langle\phi\rangle})$

$$\nabla^2\psi = \frac{G_N}{1+\alpha}4\pi\rho, \tag{6}$$

thus, the new Newtonian potential is now given by

$$\Phi_N \equiv \frac{c^2}{2}h_{00} = \psi - \frac{c^2}{2}\frac{\delta\phi}{\langle\phi\rangle}. \tag{7}$$

Solutions to these equations, the so-called potential-density pairs [54], were found for the NFW's and Dehnen's density profiles [22] and for axisymmetric systems [23]. For point particles the solution is well known, see for instance [22,50], and with the choice of the above-mentioned background field, one has

$$\Phi_N = -\frac{G_N}{1+\alpha}\frac{M}{r}(1+\alpha e^{-r/\lambda}), \tag{8}$$

where M is the point particle mass producing the field. The strength of the new scalar force is given by α and its action range by λ. For local scales, $r \ll \lambda$, deviations from the Newtonian theory are exponentially suppressed, and for $r \gg \lambda$ the Newtonian constant diminishes (augments) to $G_N/(1+\alpha)$ for positive (negative) α. Recently, the effect of STT has been investigated in different cosmological scenarios in which variations of the Newtonian constant are constrained. For instance, [55] studied the influence of varying G_N on the Doppler peaks of the cosmic microwave background radiation, and concluded that their parameter ($\xi = G/G_N$) should be in the interval $0.75 \leq \xi \leq 1.74$ in order to be within the error bars of the cosmic microwave background radiation measurements. In our notation this translates into $-0.43 \leq \alpha \leq 0.33$. However, this range for α has to be taken as a rough estimation, since these authors

have only considered a variation of G_N, and not a full perturbation study within STT. The latter has been done by [56], who found some deviations from the Newtonian dynamics, that when translated into our strength parameter would correspond to $\alpha = 0.04$; however, they do not compare their results with observations. On the other hand, a structure formation analysis has been done by [57], in which deviations of the matter power spectrum are studied by adding a Yukawa potential to the Newtonian. They found some allowed dynamics, that turn out to constrain our parameter to be within $-1.0 \leq \alpha \leq 0.5$; but again a self-consistent perturbation study in general STT is missing. Thus, the above three estimates can be taken as order-of-magnitude constraints for our models. For definiteness, we will take values within the range $-0.3 \leq \alpha \leq 3$. The value $\alpha = -0.3$ yields an asymptotic growing factor of 1.4 in G_N, whereas the value $\alpha = 3.0$ makes G_N to asymptotically reduce by one-fourth.

III. A GALACTIC MODEL

We proceed to build a galactic model by assuming that the total matter content consists of two components, baryons and cold DM, $\rho_T = \rho_{\rm B} + \rho_{\rm DM}$; Baryons represent stars, and the cold DM component could be of any type. The dynamics is determined by the theory explained in the preceding section. There are two possibilities on the DM origin: i) DM is not related to the SF, and ii) DM is associated with the boson produced by the SF. In the former case, DM can be, for example, an ensemble of neutralinos, whose mass is in the range 200 GeV $< m_\nu <$ 300 GeV [58], within an effective supergravity theory that nonminimally couples to gravity, see for example [59]. In the latter case, ii), the mass of the DM particle is given by $M_{\rm DM} = h/\lambda c$, with $\lambda \sim$ kpc, implying that $M_{\rm DM} \sim 10^{-26}$ eV. The smallness of this mass would have to be explained by a particle physics theory, e.g. similar to light scalar presented by [60], yet nonminimally coupled to gravity.

Both baryons and DM "feel" the same gravitational potential, Φ_N, but are differently distributed in the galaxy. For the baryon component we assume a Freeman-disk density profile [61,62], that is,

$$\rho_B(r) = \frac{M_d}{2\pi r_d^2} e^{-r/r_d}, \tag{9}$$

where M_d is the mass of the disk and r_d its radius.

For the DM density we do not assume a particular profile. Instead, we proceed to find its form by imposing a general rotation pattern. In the past attempts have been made to determine a universal rotation curve (URC) profile, beginning with the pioneering work of Ref. [63]. In the nineties, the authors of Refs. [64,65] considered more than 1100 optical and radio data of Sb-Im spirals to find a phenomenological URC profile valid up to the outermost radius where data were available at that time. Recently, they have considered more data and have modified the profile [66], extending it out to its virial radius, that is, including the DM halo part. This profile is supposed to be valid for spirals of different types [67] but a number of issues are still open [66]. Accordingly, we assume for our model that stars and DM particles obey the following URC profile [66]:

$$\begin{aligned} v_{\rm URC}^2 &= v_{\rm URCD}^2 + v_{\rm URCH}^2 \\ &= \frac{GM_d}{2r_d}\left(\frac{r}{r_d}\right)^2\left[I_0\left(\frac{r}{2r_d}\right)K_0\left(\frac{r}{2r_d}\right) - I_1\left(\frac{r}{2r_d}\right)K_1\left(\frac{r}{2r_d}\right)\right] + \frac{2\pi G\rho_0 r_0^3}{r}\left\{\ln\left(1+\frac{r}{r_0}\right) + \frac{1}{2}\ln\left[1+\left(\frac{r}{r_0}\right)^2\right] - \arctan\left(\frac{r}{r_0}\right)\right\} \\ &= r\frac{d\Phi_N}{dr}, \end{aligned} \tag{10}$$

where the functions I and K are the modified Bessel functions, and ρ_0 and r_0 are the scaling density and radius of the Burkert density profile [68]. The first part accounts for the disk contribution and the second for the halo's. In a previous work we have assumed a simpler, flat rotation curve profile [53].

The given circular velocity determines the form of gravitational potential Φ_N, through Eq. (10), which in turn is related to $\rho_{\rm dm}$ and $\delta\phi$ through Eqs. (4), (5), and (7).

Integrating Eq. (10) for Φ_N yields

$$\begin{aligned} \Phi_N &= \Phi_{ND} + \Phi_{NH} \\ &= -\frac{1}{2}\frac{GM_d}{r_d}\frac{r}{r_d}\left[I_0\left(\frac{r}{2r_d}\right)K_1\left(\frac{r}{2r_d}\right) - I_1\left(\frac{r}{2r_d}\right)K_0\left(\frac{r}{2r_d}\right)\right] \\ &\quad + \frac{2\pi G\rho_0 r_0^3}{r}\left\{\left(1+\frac{r}{r_0}\right)\left[\arctan\left(\frac{r}{r_0}\right) - \ln\left(1+\frac{r}{r_0}\right)\right] + \frac{1}{2}\left(-1+\frac{r}{r_0}\right)\ln\left(1+\frac{r^2}{r_0^2}\right)\right\}, \end{aligned} \tag{11}$$

TABLE I. Properties and best fitting parameters of the galaxies used.

Galaxy	Type	r_d [kpc]	M_d [$M_\odot$]	r_0 [kpc]	ρ_0 [$M_\odot$/kpc^3]	$\chi^2_{\rm red}$
DDO 47	IB	0.5	$3.60 \pm 0.62 \times 10^7$	5.43 ± 0.09	$2.67 \pm 0.03 \times 10^7$	1.74
ESO 116 − *G*12	SBcd	1.7	$2.09 \pm 0.08 \times 10^9$	4.77 ± 0.03	$4.44 \pm 0.04 \times 10^7$	0.99
NGC 7339	SABd	1.5	$1.10 \pm 0.01 \times 10^{10}$	3.03 ± 0.03	$1.60 \pm 0.02 \times 10^8$	1.69
UGC 4325	SA	1.6	$8.42 \pm 0.47 \times 10^8$	40.54 ± 10.16	$6.59 \pm 0.08 \times 10^7$	3.56

which leads to the motion of test particles in the Galaxy. Substituting this result in the original system, Eqs. (4) and (5) transform into the following two equations:

$$\nabla^2 \delta\phi - \frac{m^2}{(1+\alpha)}\delta\phi = -\frac{2\alpha}{G_N}\nabla^2\Phi_N, \tag{12}$$

$$\rho_{\rm DM} = -\rho_B + \frac{1}{4\pi G_N}\nabla^2\Phi_N + \frac{1}{8\pi(1+\alpha)}\left(\frac{mc}{h}\right)^2\delta\phi = \frac{\rho_0 r_0^3}{(r+r_0)(r^2+r_0^2)} + \frac{1}{8\pi(1+\alpha)}\left(\frac{mc}{h}\right)^2\delta\phi \tag{13}$$

for two variables, $\rho_{\rm DM}$ and $\delta\phi$. The second equality of Eq. (13) results since the disk contribution of Laplacian of Φ_N cancels out with baryon density, see Eq. (11). Thus, the resulting DM profile is the Burkert profile plus the SF contribution. By substituting Eq. (11) into Eq. (12), one solves for the scalar perturbation. Then, using Eq. (13) one solves for the DM profile. The results depend on the STT parameters (λ, α) and on the rotation curve fitting parameters (ρ_0, r_0, M_d, r_d). Particular galaxies fix the latter parameters. As an example, we had chosen a set of four galaxies of different types that have been used to test particular gravity theories [28] and to test the validity of some density profiles [36,69]. The galaxies are DD047, ESO 116-G12, NGC 7339, and UGC 4325. A greater galaxy set could have been used to test the rotation profile given by Eq. (10), but this has already been done in

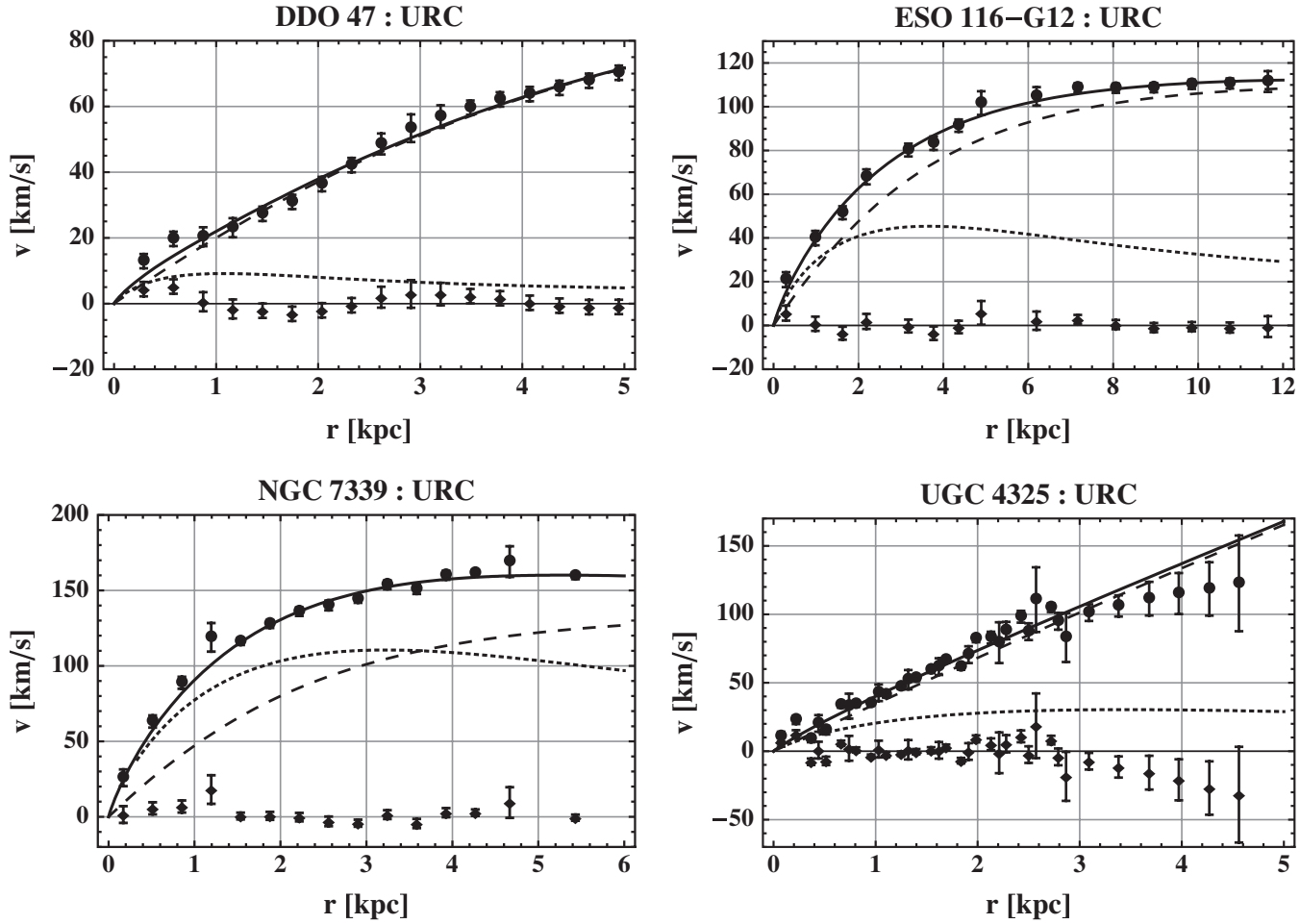

FIG. 1. The continuous line is the fitted rotation curve for data of the four galaxies. The short-dashed line is the exponential disk contribution and the long-dashed line is DM's. At the bottom we plotted the residuals ($v_{\rm obs} - v_{\rm URC}$).

Ref. [36], and in Ref. [66] additional arguments are given in favor of this rotation profile. In general, flat density profiles, such as Burkert's, tend to match rotation curves data within Newtonian dynamics [36]. In Table I, we present the properties and best fitted values of the galaxies' parameters, and in Fig. 1 the best fits are shown. The rotation curve data fit quite well to the profile URC given by Eq. (10). In doing the fitting we have taken the values for r_d, which is directly measured by optical observations, given in Ref. [70] for the first three galaxies and the values given in ref. [69] for UGC 4325. Then, we have varied M_d, r_0 and ρ_0.

The first term of the right-hand side of Eq. (13) is the Burkert profile, $\rho_{\rm BUR} \equiv \rho_0 r_0^3/(r + r_0)(r^2 + r_0^2)$ and one can define $\rho_\phi \equiv \frac{1}{8\pi(1+\alpha)}(\frac{mc}{h})^2\delta\phi$ so that to express Eq. (13) as $\rho_{\rm DM} = \rho_{\rm BUR} + \rho_\phi$. The density ρ_ϕ is the contribution of the SF fluctuation to the total density. Given this, the total density is $\rho_T = \rho_B + \rho_{\rm DM} = \rho_B + \rho_{\rm BUR} + \rho_\phi$. In what follows we proceed to numerically integrate the above equations.

IV. SPHERICAL SOLUTION

Unfortunately, these quantities cannot be computed analytically, since the Newtonian potential involves cylindrical and spherical dependencies. Therefore, to solve the Eq. (12) we will assume spherical symmetry. Then, we use the integrals given in Ref. [22] to numerically solve for $\delta\phi$.

We perform the integration for the low surface brightness galaxy UGC 4325; because the NFW model does not properly fit with the observations, so we plan for this galaxy to contrast our results with them.

Let us explain the range of values for the STT parameters taken in our analysis. Originally, STT [47,48] were thought for positives values of α to have a standard kinetic term in Eq. (1). But negatives values are also theoretically possible [71,72] and they have been applied, for instance, to accomplish, without a potential in Eq. (1), an inflationary era in isotropic [73] and anisotropic models [74], or more recently, to explain the present accelerated expansion of the Universe in some quintessence models [75,76]. Thus, we will consider positive as well negative values of α subject to the constraints mentioned at the end of Sec. II. Therefore, we will analyze the solutions in the interval $-0.3 \leq \alpha \leq 3.0$. On the other hand, we will assume that λ is in the interval 0.1 kpc $\leq \lambda \leq$ 50 kpc to fit galactic scales.

A. Solutions for positive α

In Fig. 2(a) we plot the resulting density profiles for $\alpha = 3.0$ and $\lambda = 1.0$ kpc. Of particular interest is the form of the DM profile that flattens near the center of the Galaxy. The latter is again shown in Fig. 2(b), where for comparison the standard Newtonian density profile ρ_N is plotted,

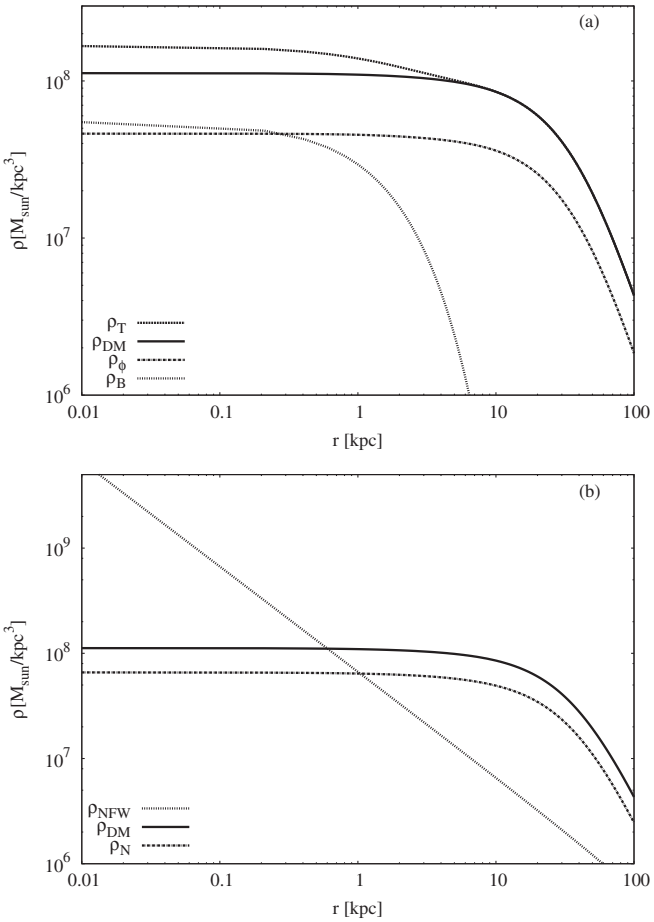

FIG. 2. (a) It is shown all density profiles using $\alpha = 3.0$ and $\lambda = 1$ kpc. (b) It is shown $\rho_{\rm NFW}$, $\rho_{\rm DM}$ and ρ_N for comparison.

which is the profile to have $v^2_{\rm URCH}$ as given by Eq. (10), but turning off the SF; i.e., ρ_N is the density found by solving the Poisson equation with Newtonian potential given by Φ_{NH} in Eq. (11). Thus, the Newtonian density is the Burkert profile [68]. One observes that $\rho_{\rm DM}$ is always bigger than ρ_N, since the effect of the SF is to diminish the effective gravitational constant for $r > \lambda$, since $G_{\rm eff} = G(1 + \alpha e^{-r/\lambda})/(1 + \alpha)$, thus to compensate the reduction of the gravitational constant, a denser DM profile is necessary to have the same rotation curve profile. Concerning the behavior of the profile, we have computed a numerical fit of the inner part of the curve ($r \ll r_d$), showing that it behaves approximately as $\rho_{\rm DM} \sim r^{-\gamma_{\rm DM}}$ with $\gamma_{\rm DM} \approx 0.00\,006^{+0.00\,002}_{-0.00\,001}$; the uncertainties stemming basically from the uncertainties in r_0. On the other hand, the standard Newtonian model is just a little steeper $\rho_N \sim r^{-\gamma_N}$ with $\gamma_N \approx 0.00\,010^{+0.00\,003}_{-0.00\,002}$. Both of these profiles are essentially shallow. The NFW that best fitted rotation curves data is included for comparison, which is known to be cuspier in the inner region, $\rho_{\rm NFW} \sim r^{-1.00\,001}$. For $r \sim r_d$ the behavior follows $\rho_{\rm DM} \sim r^{-\delta_{\rm DM}}$ with $\delta_{\rm DM} \approx 0.040^{+0.011}_{-0.007}$, $\rho_N \sim r^{-\delta_N}$ with $\delta_N \approx 0.041^{+0.014}_{-0.008}$. The NFW

model behaves as $\rho_{\rm NFW} \sim r^{-\delta_{\rm NFW}}$ with $\delta_{\rm NFW} \sim 1.003$. For $r \sim r_0$ the behavior follows $\rho_{\rm DM} \sim r^{-\delta_{\rm DM}}$ with $\delta_{\rm DM} \approx 1.44^{+0.34}_{-0.26}$, $\rho_N \sim r^{-\delta_N}$ with $\delta_N \approx 1.44^{+0.34}_{-0.26}$, and the NFW model behaves as $\rho_{\rm NFW} \sim r^{-\delta_{\rm NFW}}$ with $\delta_{\rm NFW} \sim 1.08$. Figure 2(b) shows that the DM profile is bigger than NFW's beyond $r \sim 0.6$ kpc. On the other hand, Ref. [69] shows that NFW fits are bad for this galaxy, because arbitrary low concentrations (i.e., large NFW scaling length r_s) are needed. In our case, the best fitted curve implies a concentration $c = 1.22$, which is clearly inconsistent with the cosmological expected values $c > 5$ (for a wide range of v_{200} values) [9,77]. Thus, what we essentially see in our plots of the NFW profile is its cuspy region, as shown in Fig. 2(b).

The solution shown for the SF is the interior solution and eventually at some $r = R$ the exterior solution is valid [22]; one could think of R to be of the order of the halo size. Thus, for $r \geq R$, the SF exponentially vanishes and we obtain a standard Newtonian behavior. Therefore, asymptotically, for $r \gg r_0$, $\rho_{\rm DM} \sim r^{-3}$ similar to $\rho_{\rm NFW} \sim r^{-3}$.

In Figs. 3(a) and 3(b) we have plotted the SF and DM profiles for various λ. The SF fluctuation diminishes going from the center to outer parts, and for smaller λ the decay is stronger in inner regions. Figure 3(a) shows also that the SF is bigger for larger λ, since for large λ, $G_{\rm eff}$ approaches to G. A consistency check implies that the SF must comply with the condition $\delta\phi < (1+\alpha)c^2 G_N^{-1} = (1+\alpha)2.1 \times 10^{16} M_\odot/\text{kpc}$ in order to validate the perturbation theory used, and it is indeed the case for the pair of parameters (λ, α) chosen. On the other hand, the DM profiles in Fig. 3(b) diminish by augmenting λ. The DM profile more deviates from the standard Newtonian one for smaller λ.

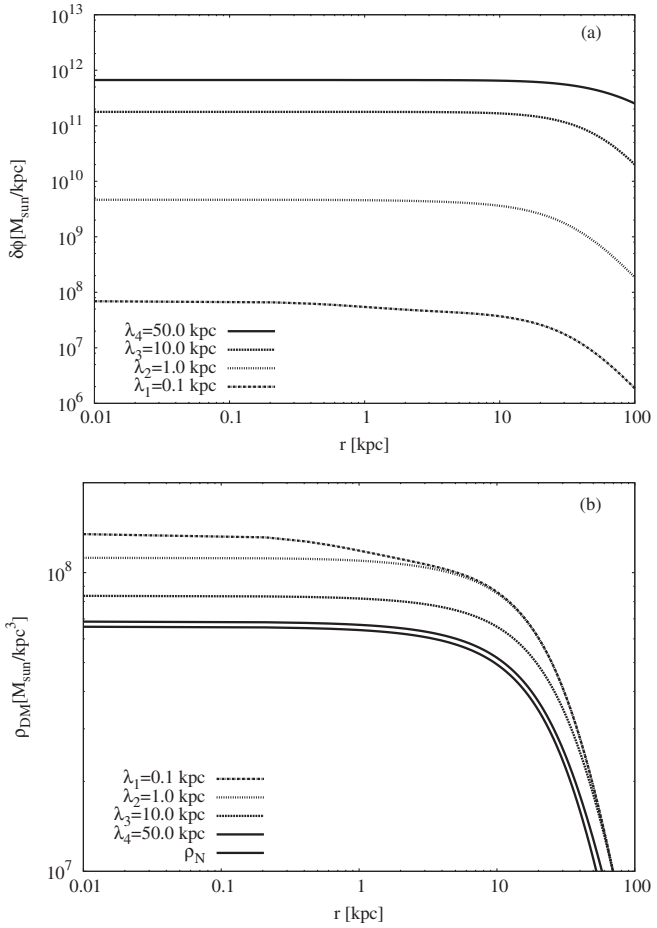

FIG. 3. (a) It is shown the SF perturbation and (b) the DM profile for various λ and fixed $\alpha = 3.0$.

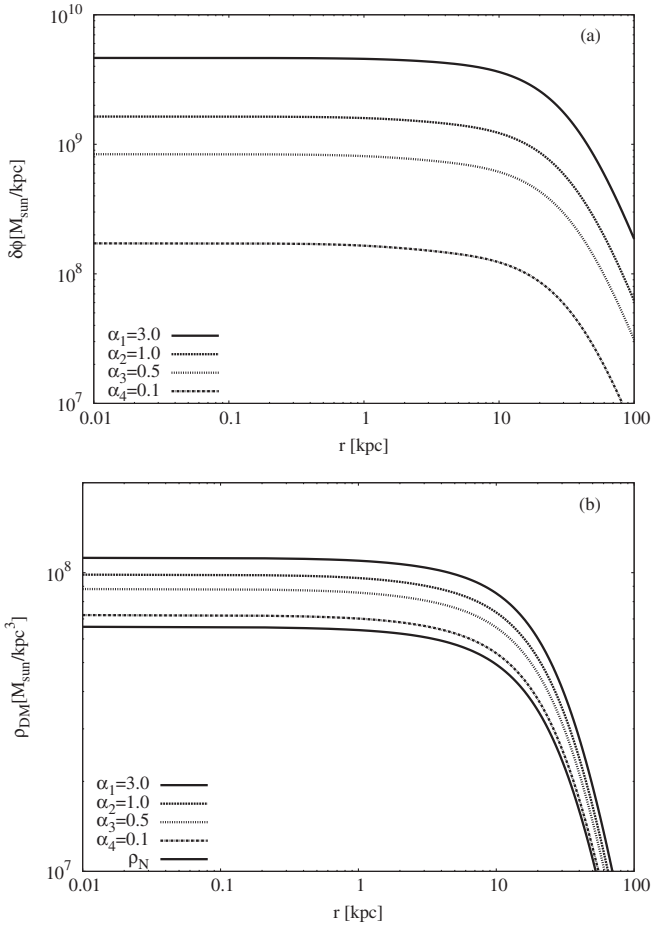

FIG. 4. (a) It is shown the SF perturbation and (b) the DM profile for various α and fixed $\lambda = 1$ kpc.

In Figs. 4(a) and 4(b) we plotted the SF and DM profiles for various α and fixed $\lambda = 1.0$ kpc. Again the constraint on $\delta\phi$ is fulfilled (Fig. 4(a)). As expected, for small α the DM profile tends to the standard Newtonian one (Fig. 4(b)).

B. Solutions for negative α

In Fig. 5(a) we again plot all densities, as in Fig. 2(a), but now for $\alpha = -0.1$ and $\lambda = 1.0$ kpc. The DM profile in the inner regions ($r \ll r_d$) is given by $\rho_{\rm DM} \sim r^{-\gamma_{\rm DM}}$ with $\gamma_{\rm DM} \approx 0.00\,011^{+0.00\,004}_{-0.00\,002}$, that is quite similar as the standard Newtonian, which gives $\rho_N \sim r^{-\gamma_N}$, with

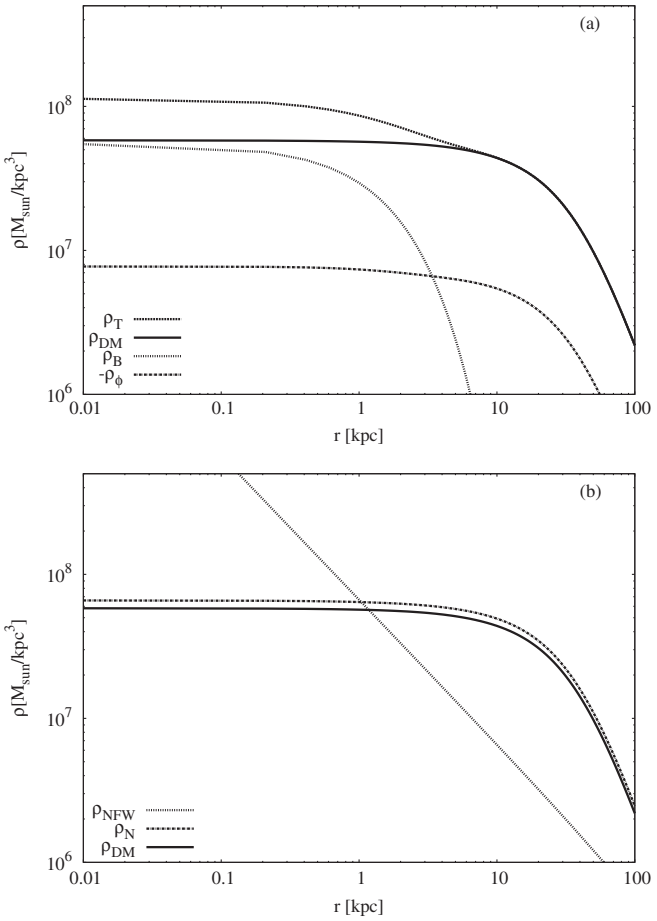

FIG. 5. (a) It is shown all density profiles using $\alpha = -0.1$ and $\lambda = 1$ kpc. (b) It is shown $\rho_{\rm NFW}$, $\rho_{\rm DM}$ and ρ_N for comparison.

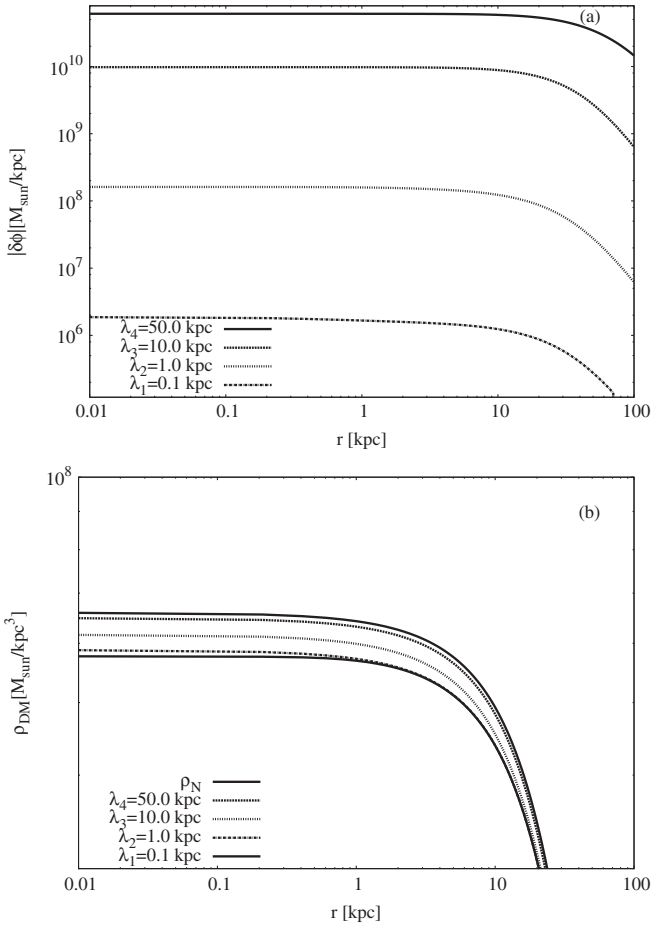

FIG. 6. (a) It is shown the SF perturbation and (b) the DM profile for various λ and fixed $\alpha = -0.1$.

$\gamma_N \approx 0.00\,010^{+0.00\,003}_{-0.00\,002}$; they are shallow. In contrast, NFW's profile in the same region that has a cuspy power $\gamma_{\rm NFW} = -1.00\,001$. Figure 5(b) shows the DM, Newtonian, and NFW profiles for comparison. It is clear that the DM profile is less massive than the standard Newtonian. This is because the effective gravitational function, $G_{\rm eff} = G(1 + \alpha e^{-r/\lambda})/(1 + \alpha)$, is increased for negative α, and the gravitational pull, being proportional to the term $G_{\rm eff}M$, is compensated by a decrease in $M(r)$, that is by a decrease of the DM profile. For $r \sim r_d$ the behavior is as follows: $\rho_{\rm DM} \sim r^{-\delta_{\rm DM}}$ with $\delta_{\rm DM} \approx 0.035^{+0.015}_{-0.009}$, the standard Newtonian profile is $\rho_N \sim r^{-\delta_N}$ with $\delta_N \approx 0.041^{+0.014}_{-0.008}$, the NFW's behaves nearly as $\delta_{\rm NFW} = 1.00$. For $r \sim r_0$ the behavior follows $\rho_{\rm DM} \sim r^{-\delta_{\rm DM}}$ with $\delta_{\rm DM} \approx 1.44^{+0.34}_{-0.26}$, $\rho_N \sim r^{-\delta_N}$ with $\delta_N \approx 1.44^{+0.34}_{-0.26}$, the NFW model behaves as $\rho_{\rm NFW} \sim r^{-\delta_{\rm NFW}}$ with $\delta_{\rm NFW} \sim 1.08$. As in the α-positive case, Fig. 5(b) shows again that beyond some region ($r \sim 1$ kpc) the DM profile is bigger than NFW's. Asymptotically, for $r \gg r_0$, beyond some point the exterior solution is valid, thus $\rho_{\rm DM} \sim r^{-3}$, similar to $\rho_{\rm NFW} \sim r^{-3}$.

Figures 6(a) and 6(b) show the SF and DM profiles for various λ, respectively. The behaviors show systematic tendencies: the smaller λ, the smaller $|\delta\phi|$, and again and for smaller λ, the decay is stronger in inner regions (Fig. 6(a)). The SF complies with $\delta\phi < (1 + \alpha)c^2 G_N^{-1}$, guaranteeing the validity of the perturbation approach. On the other hand, the bigger λ, the closer the DM profile approaches to the standard Newtonian model (Fig. 6(b)).

In Figs. 7(a) and 7(b) we plotted the SF and DM profiles for various negative α and fixed $\lambda = 1.0$ kpc. Again, the constraint on $\delta\phi$ is fulfilled. As expected, for smaller $|\alpha|$ the DM profile tends to the standard Newtonian one ($\alpha = 0$).

V. DISCUSSION AND CONCLUSIONS

We have considered a general STT in its weak energy limit in which two free parameters appear (λ, α). This pair can be constrained by the above-mentioned observations: the first parameter is the Compton wavelength associated with a light boson particle, which we have taken to be of the order of kiloparsecs; this value implies a change of the Newtonian constant only at distances of the order of galactic scales or bigger, and therefore does not conflict with local deviations of Newtonian dynamics [78]. The other parameter is the strength of the new scalar force, given by

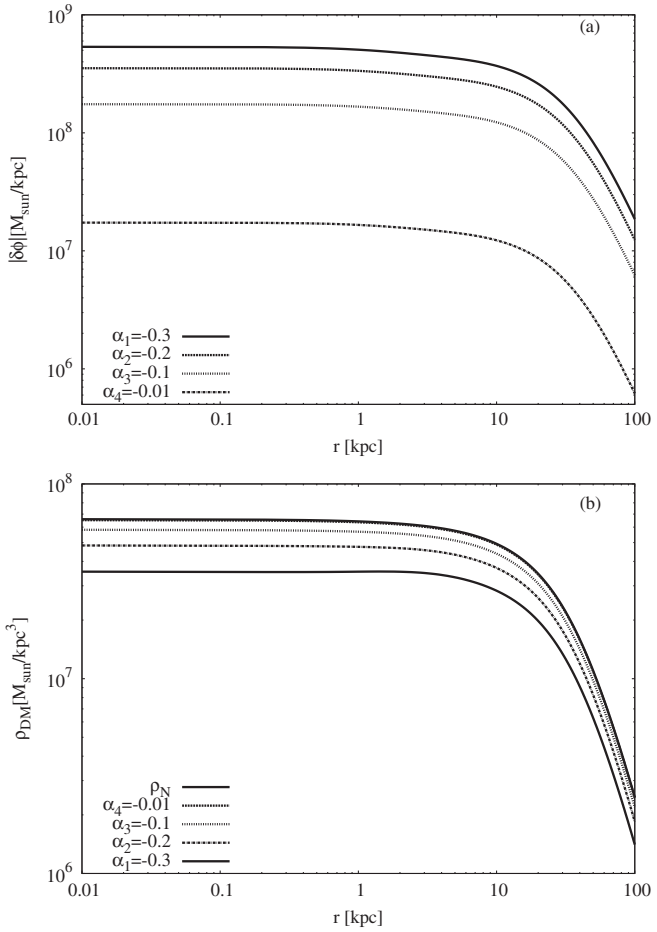

FIG. 7. (a) It is shown the SF perturbation and (b) the DM profile for various negative α and fixed $\lambda = 1$ kpc.

α, which is subject to cosmological constraints. Accordingly, we have taken values for α within the range $-0.3 \leq \alpha \leq 3$. We do not use bigger positive (negative) values for α because they predict a weaker (stronger) gravitational constant on scales larger than λ, and bring some unacceptable cosmological effects [55–57].

Using the STT formalism, we have constructed a galactic model with a distribution of stars and DM that obey a rotation profile compatible with observations given by the URC of [66], as is shown in Fig. 1. This fitting determines the form of the effective gravitational potential Φ_N, given by Eq. (11). Then, by taking a typical density profile for baryons (Freeman exponential profile), the only two quantities to be determined are the SF fluctuation and DM profile, which are given by Eqs. (12) and (13), respectively, for which we have found numerical solutions.[1] In a previous work [53] we have found analytic solutions for a flat rotation curve profile. Those solutions are similar to NFW's [25]. The numerical solutions found here are shallow near the galaxy center, since the universal rotation curve of the halo (URCH), Eq. (10), stems from the Burkert profile [68], which is shallow for $r \ll r_0$. In order to make a comparison with the standard Newtonian model, we turned off the SF and solved for the density in the standard Poisson using Eq. (11). The resulting profile is called ρ_N and is the well-known Burkert profile. The DM profile found here is slightly shallower (cuspier) than the Newtonian profile for positive (negative) values of α, and in any case much shallower than NFW's. To quantitatively analyze the solutions we have considered the two scales involved in the URC fitting, that are the disc radius, r_d, and the DM scale, r_0. The DM solutions near the galactic center ($r \ll r_d$) with α positive are a bit shallower ($\rho \sim r^{-0.00\,006^{+0.00\,002}_{-0.00\,001}}$) than those with α negative ($\rho \sim r^{-0.00\,011^{+0.00\,004}_{-0.00\,002}}$), and both of them are much shallower than NFW's profiles [25,29,31,33]. Solutions at $r \sim r_d$ for α positive decay as ($\rho_{\rm DM} \sim r^{-0.040^{+0.011}_{-0.007}}$) and for α negative decay weaker ($\rho \sim r^{-0.035^{+0.015}_{-0.009}}$). At $r \sim r_0$ for positive α the DM profile behaves as $\rho \sim r^{-1.44^{+0.34}_{-0.26}}$ and for negative α the behavior is $\rho \sim r^{-1.44^{+0.34}_{-0.26}}$. The uncertainties stemming from the allowed values of the fitting parameters reported in Table I. For the allowed values of r_0, the DM exponents for $r \ll r_d$ vary between 20%–34%, for $r \sim r_d$ between 17%–29%, and for $r \gg r_d$ vary between 18%–24%. The slopes of the DM profiles change smoothly, so that their behavior does not qualitatively differ from their mean value. With respect to the variations of M_d and ρ_0, the exponents vary less than (or of the order of) 1%.

On the other hand, for positive (negative) α, $\rho_{\rm DM}$ is bigger (smaller) than ρ_N always, since the effect of the SF is to diminish (augment) the effective gravitational constant for $r > \lambda$, being $G_{\rm eff} = G(1 + \alpha e^{-r/\lambda})/(1 + \alpha)$, thus it is necessary to compensate it with a corresponding larger (smaller) DM density. Finally, asymptotically, for $r \gg r_0$, the exterior solution is valid, and thus $\rho_{\rm DM} \sim r^{-3}$ is similar to $\rho_{\rm NFW} \sim r^{-3}$.

We have found numerical solutions for the allowed parameter space for strength of the SF potential, $-0.3 \leq \alpha \leq 3.0$, and within galactic distances, 0.1 kpc $\leq \lambda \leq$ 50 kpc. The results indicate some systematic tendencies: the effect of the SF is more apparent for $\lambda < r_0$, and its influence attenuates for $\lambda > r_0$, since in this regime the behavior is essentially Newtonian ($\lambda = \infty$) for $r < r_0$. For small $|\alpha|$ the DM profile tends to the standard Newtonian one ($\alpha = 0$).

The intention of the present work was to study the influence of a massive SF in a galaxy model that is compatible with a typical baryon distribution and follows the URC of observed galaxies. This construction fixes the Newtonian potential, and for the STT parameters analyzed, the resulting DM profile is shallow at the center of the halo.

[1] In other models, such as the gravitational suppression hypothesis [27] one assumes a NFW DM profile to determine the parameters (λ, α) of that theory by fitting theoretical curves to the rotation curves data [28]. In our approach, we determine the DM profile by setting a fitted universal rotation curve that is generic for different spiral types [66].

These results are encouraging showing the important role that both contributions, DM and STT, could have in the dynamics of the systems. We think that numerical N-body simulations using the STT of gravity have to be done to confirm the solutions discussed here. Some preliminary computations have been carried out in Refs. [79,80].

ACKNOWLEDGMENTS

This work was supported by CONACYT Grant Nos. 84133-F, U47209-F, and I0101/131/07 C-234/07. We thank P. Salucci and R. Kuzio de Naray and collaborators [69] for providing us with the rotation curves data used here.

[1] C. L. Bennett *et al.*, Astrophys. J. Suppl. Ser. **148**, 1 (2003).
[2] P. de Bernardis *et al.*, Nature (London) **404**, 995 (2000).
[3] G. Efstathiou, Mon. Not. R. Astron. Soc. **330**, L29 (2002).
[4] G. Hinshaw *et al.*, Astrophys. J. Suppl. Ser. **180** 225 (2009).
[5] J. A. Peacock, in *A New Era in Cosmology, ASP Conference Proceedings*, edited by T. Shanks and N. Metcalfe (Astronomical Society of the Pacific, San Francisco, 2002), Vol. 283, p. 19.
[6] S. Perlmutter *et al.*, Astrophys. J. **517**, 565 (1999).
[7] A. G. Riess *et al.*, Astron. J. **116**, 1009 (1998).
[8] A. G. Riess *et al.*, Astrophys. J. **560**, 49 (2001).
[9] D. N. Spergel *et al.*, Astrophys. J. Suppl. Ser. **170**, 377 (2007).
[10] L. Amendola, Phys. Rev. Lett. **86**, 196 (2001).
[11] B. Boisseau, G. Esposito-Farese, D. Polarski, and A. A. Starobinsky, Phys. Rev. Lett. **85**, 2236 (2000).
[12] R. R. Caldwell, R. Dave, and P. J. Steinhardt, Phys. Rev. Lett. **80**, 1582 (1998).
[13] M. Gasperini and G. Veneziano, Phys. Rep. **373**, 1 (2003).
[14] M. B. Green, J. H. Schwarz, and E. Witten, *Superstring Theory* (Cambridge University Press, Cambridge, 1988).
[15] J. P. Ostriker and P. J. E. Peebles, Astrophys. J. **186**, 467 (1973).
[16] R. H. Sanders, Astron. Astrophys. **136**, L21 (1984).
[17] M. Milgrom, Astrophys. J. **270**, 365 (1983).
[18] R. H. Sanders and S. S. McGaugh, Annu. Rev. Astron. Astrophys. **40**, 263 (2002).
[19] T. Matos and F. S. Guzman, Classical Quantum Gravity **18**, 5055 (2001).
[20] T. Matos, F. S. Guzman, and D. Núñez, Phys. Rev. D **62**, 061301(R) (2000).
[21] A. Aguirre, C. P. Burgess, A. Friedland, and D. Nolte, Classical Quantum Gravity **18**, R223 (2001).
[22] M. A. Rodríguez-Meza and J. L. Cervantes-Cota, Mon. Not. R. Astron. Soc. **350**, 671 (2004).
[23] M. A. Rodríguez-Meza *et al.*, Gen. Relativ. Gravit. **37**, 823 (2005).
[24] N. M. Bezares-Roder and H. Dehnen, Gen. Relativ. Gravit. **39**, 1259 (2007).
[25] J. F. Navarro *et al.*, Astrophys. J. **462**, 563 (1996); **490**, 493 (1997).
[26] W. Dehnen, Mon. Not. R. Astron. Soc. **265**, 250 (1993).
[27] F. Piazza and C. Marinoni, Phys. Rev. Lett. **91**, 141301 (2003).
[28] C. F. Martins and P. Salucci, Phys. Rev. Lett. **98**, 151301 (2007).
[29] E. Hayashi *et al.*, Mon. Not. R. Astron. Soc. **355**, 794 (2004).
[30] A. Mahdavi and M. J. Geller, Astrophys. J. **607**, 202 (2004).
[31] J. F. Navarro *et al.*, Mon. Not. R. Astron. Soc. **349**, 1039 (2004).
[32] E. Pointecouteau, M. Arnaud, J. Kaastra, and J. de Plaa, Astron. Astrophys. **423**, 33 (2004).
[33] C. Power, J. F. Navarro, A. Jenkins, C. S. Frenck, S. D. M. White, V. Springel, J. Stadel, and T. Quinn, Mon. Not. R. Astron. Soc. **338**, 14 (2003).
[34] J. J. Binney and N. Evans, Mon. Not. R. Astron. Soc. **327**, L27 (2001).
[35] F. Donato, G. Gentile, and P. Salucci, Mon. Not. R. Astron. Soc. **353**, L17 (2004).
[36] G. Gentile, P. Salucci, U. Klein, D. Vergani, and P. Kalberla, Mon. Not. R. Astron. Soc. **351**, 903 (2004).
[37] G. Gentile, A. Burkert, P. Salucci, U. Klein, and F. Walter, Astrophys. J. **634**, L145 (2005).
[38] G. Gentile, P. Salucci, U. Klein, and G. L. Granato, Mon. Not. R. Astron. Soc. **375**, 199 (2007).
[39] P. Salucci, Mon. Not. R. Astron. Soc. **320**, L1 (2001).
[40] D. J. Sand, T. Treu, G. P. Smith, and R. S. Ellis, Astrophys. J. **604**, 88 (2004).
[41] J. D. Simon, A. D. Bolatto, A. Leroy, L. Blitz, and E. L. Gates, Astrophys. J. **621**, 757 (2005).
[42] R. A. Swaters, B. F. Madore, F. C. van den Bosch, and M. Balcells, Astrophys. J. **583**, 732 (2003).
[43] F. C. van den Bosch and R. A. Swaters, Mon. Not. R. Astron. Soc. **325**, 1017 (2001).
[44] B. J. Weiner, J. A. Sellwood, and T. B. Williams, Astrophys. J. **546**, 931 (2001).
[45] D. T. F. Weldrake, W. J. G. de Blok, and F. Walter, Mon. Not. R. Astron. Soc. **340**, 12 (2003).
[46] K. Spekkens, R. Giovanelli, and M. P. Haynes, Astron. J. **129**, 2119 (2005).
[47] C. Brans and R. H. Dicke, Phys. Rev. **124**, 925 (1961).
[48] R. V. Wagoner, Phys. Rev. D **1**, 3209 (1970).
[49] J. L. Cervantes-Cota, M. A. Rodríguez-Meza, R. Gabassov, and J. Klapp, Rev. Mex. Phys. S **53**, 22 (2007).
[50] T. Helbig, Astrophys. J. **382**, 223 (1991).
[51] K. Nordtvedt, Jr., Astrophys. J. **161**, 1059 (1970).
[52] C. M. Will, *Theory and Experiment in Gravitational Physics* (Cambridge University Press, Cambridge, 1992), 2nd ed..
[53] J. L. Cervantes-Cota, M. A. Rodríguez-Meza, and D. Núñez, J. Phys. Conf. Ser. **91**, 012007 (2007).
[54] J. Binney and S. Tremaine, *Galactic Dynamics* (Princeton

Univ. Press, Princeton, NJ, 2008), 2nd ed..
[55] K. I. Umezu, K. Ichiki, and M. Yahiro, Phys. Rev. D **72**, 044010 (2005).
[56] R. Nagata, T. Chiba, and N. Sugiyama, Phys. Rev. D **66**, 103510 (2002).
[57] A. Shirata, T. Shiromizu, N. Yoshida, and Y. Suto, Phys. Rev. D **71**, 064030 (2005).
[58] L. G. Cabral-Rosetti, X. Hernández, and R. A. Sussman, in *The Early Universe and Obsevational Cosmology*, Lectures Notes in Physics Vol. 646, edited by N. Breton, J. L. Cervantes-Cota, and M. Salgado (Springer, Berlin Heidelberg, 2004), p. 309.
[59] R. A. El-Nabulsi, Phys. Lett. B **619**, 26 (2005).
[60] S. M. Carroll, Phys. Rev. Lett. **81**, 3067 (1998).
[61] J. N. Bahcall and R. M. Soneira, Astrophys. J. Suppl. Ser. **44**, 73 (1980).
[62] K. Freeman, Astrophys. J. **160**, 811 (1970).
[63] V. C. Rubin, D. Burstein, W. K. Ford, Jr., and N. Thonnard, Astrophys. J. **289**, 81 (1985).
[64] M. Persic and P. Salucci, Astrophys. J. **368**, 60 (1991).
[65] M. Persic, P. Salucci, and F. Stel, Mon. Not. R. Astron. Soc. **281**, 27 (1996).
[66] P. Salucci, A. Lapi, C. Tonini, G. Gentile, I. Yegorova, and U. Klein, Mon. Not. R. Astron. Soc. **378**, 41 (2007).
[67] P. Salucci and M. Persic, in Astron. Soc. Pac. Conf. Ser. **117**, 1 (1997).
[68] A. Burkert, Astrophys. J. **447**, L25 (1995).
[69] R. Kuzio de Naray, S. S. McGaugh, and W. J. G. de Blok, Astrophys. J. **676**, 920 (2008).
[70] C. F. Martins and P. Salucci, Mon. Not. R. Astron. Soc. **381**, 1103 (2007).
[71] H. P. Nilles, Phys. Rep. **110**, 1 (1984).
[72] M. D. Pollock, Phys. Lett. B **215**, 635 (1988).
[73] J. J. Levin, Phys. Rev. D **51**, 462 (1995).
[74] J. L. Cervantes-Cota, Classical Quantum Gravity **16**, 3903 (1999).
[75] R. R. Caldwell, Phys. Lett. B **545**, 23 (2002).
[76] M. P. Dabrowski, T. Stachowiak, and M. Szydlowski, Phys. Rev. D **68**, 103519 (2003).
[77] M. Tegmark *et al.*, Phys. Rev. D **69**, 103501 (2004).
[78] E. Fischbach and C. L. Talmadge, *The Search for Non-Newtonian Gravity* (Springer-Verlag, New York, 1999).
[79] M. A. Rodríguez-Meza, A. X. González-Morales, R. F. Gabbasov, and J. L. Cervantes-Cota, J. Phys. Conf. Ser. **91**, 012012 (2007).
[80] M. A. Rodríguez-Meza, in *Recent Developments in Gravitation and Cosmology: 3rd. Mexican Meeting on Mathematical and Experimental Physics*, edited by A. Macías, C. Laemmerzahl, and A. Camacho, AIP Conf. Proc. (AIP, New York, 2008), Vol. 977, p. 302.